Journal of Materials Chemistry A

RSC Publishing

PAPER

View Article Online
View Journal | View Issue

Graphene-supported $Na_3V_2(PO_4)_3$ as a high rate cathode material for sodium-ion batteries

Cite this: *J. Mater. Chem. A*, 2013, **1**, 11350

Young Hwa Jung, Chek Hai Lim and Do Kyung Kim*

Received 30th May 2013
Accepted 17th July 2013

DOI: 10.1039/c3ta12116j

www.rsc.org/MaterialsA

Substantial interest in sodium resources that are inexpensive and abundant in the earth has guided intense research on Na-based electrode materials. We report a facile synthetic strategy to improve the rate performance of Na-based electrode materials in sodium-ion batteries. $Na_3V_2(PO_4)_3$ (NVP) is one of the most promising cathode materials with a NASICON structure, and it has been synthesized on a graphene sheet surface using a simple method that combines sol–gel and solid-state reaction. The NVP/graphene composite displays an excellent high-rate performance; it delivers approximately 67% of the initial 0.2 C capacity at a 30 C rate, whereas bare NVP produces only 46% of the 0.2 C capacity at a 5 C rate. It also demonstrates high capacity retention both at 1 C and 10 C cycles as a promising cathode for rechargeable sodium-ion batteries. This outstanding result can be ascribed to the key role of graphene in enhancing the electronic conductivity of electrode materials compared with bare NVP.

Introduction

Energy conversion and storage materials that can replace fossil fuels have received considerable attention as concerns over global warming have grown. Among several energy storage systems, lithium-ion batteries (LIBs) have been widely accepted for high energy density and a long lifetime.[1,2] The widespread application of LIBs has increased the demand for lithium resources; as a result, it is debatable whether the cost of lithium would be sufficiently low for application in broader markets such as electric vehicles (EVs) and energy storage systems.[3] Thus, scientific research on sodium-based batteries, which are advantageous due to abundance and low cost, has rapidly risen as lithium alternatives.[4–6] Most sodium-based electrode materials, however, have shown low C-rate performances regardless of the crystal structures.[7–11] The rate problem for sodium-ion batteries may be intrinsic in view of a larger Na^+ size (1.02 Å) compared with Li^+ (0.76 Å), and this issue may prevent sodium batteries from being used in EVs and large energy storage systems. To improve the rate characteristics of Na electrode materials, a traditional carbon coating method has been adopted in solid state synthesis using carbon sources.[11–16] Although this attempt has been effective to a certain degree, the higher rate (over 2 C) capacity remains low. Therefore, it is necessary to overcome the rate problem in sodium-based electrode materials.

Graphene, a two-dimensional (2D) form of carbon allotrope, is the basic building unit of all graphitic materials (fullerenes, carbon nanotubes, graphite, *etc.*). It has been utilized for several applications such as energy storage/conversion materials and micro/optoelectronic devices due to its remarkably high electronic, optical, thermal and mechanical properties as well as a unique structure.[17–19] Among these applications, graphene has been used to form composites or hybrids as a highly electronic conductive network in the fields of rechargeable batteries.[19–21] While many groups have previously demonstrated the effect of graphene in LIBs,[21] sodium-based electrode materials with graphene have rarely been reported.

In this work, we present a simple synthetic approach to attach $Na_3V_2(PO_4)_3$ (NVP) on graphene surfaces to enhance the rate performance of active materials in sodium-ion batteries. NASICON-structured materials have attracted widespread interest for high ionic conductivity;[22–26] however, it is difficult to apply such materials as electrodes in rechargeable batteries owing to poor electronic conductivity. Recently, several groups have reported the electrochemical properties of NVP as a cathode material candidate in sodium-ion batteries.[11–13,27–29] NVP exhibits a moderate voltage plateau at approximately 3.4 V and has a relatively high reversible capacity (~90 mA h g^{-1}); further, NVP's stable structure demonstrates good cyclability at a low C-rate in sodium-ion cells. Here, a highly crystalline NVP/graphene composite has been synthesized for the first time as a cathode material for rechargeable sodium-ion batteries using a simple method that combines sol–gel and solid-state reaction. Excellent rate capability of the NVP/graphene composite could be achieved even with a low graphene amount (~5 wt%); 82% of initial 0.2 C discharge capacity was retained at a 100-fold greater rate, 20 C. This result would be meaningful in that the graphene composite can also be applied as a promising high rate electrode material in a variety of sodium-based rechargeable batteries.

Department of Materials Science and Engineering, Korea Advanced Institute of Science and Technology (KAIST), 335 Gwahangno, Yuseong-gu, Daejeon, 305-701, Republic of Korea. E-mail: dkkim@kaist.ac.kr; Fax: +82 42 350 3310; Tel: +82 42 350 4118

Experimental

Synthesis of the NVP/graphene composite

Graphene oxide (GO) was prepared using a modified Hummers method as previously reported.[30,31] After washing and exfoliation of GO, the centrifuged GO was freeze dried under vacuum conditions for 2 days. 0.7564 g of oxalic acid was used as a chelating agent to react with NH_4VO_3 (2 mmol) in 80 mL of distilled water under vigorous stirring and heating at 80 °C. After 1 h, 0.045 g of freeze dried GO was dispersed into the mixture under sonication for 1 h, and the mixture was continuously stirred to produce a homogenous solution. Stoichiometric levels of $NH_4H_2PO_4$ (3 mmol) and Na_2CO_3 (1.5 mmol) were added into the solution under vigorous stirring and heating at 80 °C until they were dried. The black solid was ground and pre-calcined at 350 °C for 3 h under an N_2 atmosphere. The powder produced was re-ground and calcined at 700 °C in a N_2–H_2 mixture with 5% H_2 (v/v) for 10 h. Bare NVP was prepared through the same process except that GO was added.

Characterizations

Powder X-ray diffraction (PXRD) characterization was performed using an X-ray diffractometer (Rigaku D/Max-2500) with a Cu X-ray ($\lambda = 1.5418$ Å) at ambient temperature. Synchrotron PXRD data were collected at room temperature using Beamline 9B ($\lambda = 1.5474$ Å) at the Pohang Light Source (PLS) in Korea with a six multi-detector system over an angular range of $10° \leq 2\theta \leq 130°$ at a 0.02° step width. The crystal structure was refined using the powder profile refinement program GSAS.[32] The morphology and microstructure were characterized using scanning electron microscopy (FE-SEM, Hitachi, S-4800) and transmission electron microscopy (FE-TEM (300 kV) Tecnai G^2 F30). The structural property of the NVP/graphene composite was analyzed by Raman spectroscopy (LabRAM) and the carbon content of the sample was measured using an element analyzer (Thermo Scientific, Flash 2000 series).

Electrochemical measurement

Electrochemical tests for the NVP electrodes were performed in beaker-type cells using Na metal as the counter and reference electrodes, which were assembled in an Ar-filled glove box. The working electrode consisted of 75 wt% active material, 17 wt% carbon black, and 8 wt% PVDF on a stainless steel foil. The active material load was approximately 1 mg cm^{-2}. The electrolyte was 1 M $NaClO_4$ in propylene carbonate (PC). The galvanostatic tests were performed using a VMP3 potentiostat (Bio-Logic) at ambient temperature. The Na half-cells were tested between 2.5 V and 3.8 V *vs.* Na^+/Na at various C-rates based on the theoretical capacity of 118 mA h g^{-1}.

Results and discussion

Fig. 1(a) and (b) show PXRD patterns for bare NVP and the NVP/graphene composite, respectively. The bare NVP and NVP/graphene composite peaks are consistent with the calculated pattern for $Na_3V_2(PO_4)_3$. The peak positions, intensity ratios and peak sharpness for the two samples are similar, which indicates a crystalline phase without noticeable impurities. To confirm the NVP/graphene composite phase more precisely, a high resolution synchrotron PXRD pattern was collected, and the Rietveld refinement result is shown in Fig. 1(c). The synchrotron PXRD pattern also shows a NASICON structure in a $R\bar{3}c$ (rhombohedral, no.167) space group,[33] and the cell parameters were refined as follows: $a = 8.72457$ (5) Å and $c = 21.8039$ (3) Å ($R_p = 6.38\%$, $wR_p = 8.38\%$, $\chi^2 = 3.86$). The inset of Fig. 1(c) depicts the NASICON structure, wherein Na ions are in the Na1 (M1) and Na2 (M2) sites of channels with a corner-shared VO_6 octahedral (blue) and PO_4 tetrahedral (yellow) framework. It is well known that the Na1 site is fully occupied and two-third of

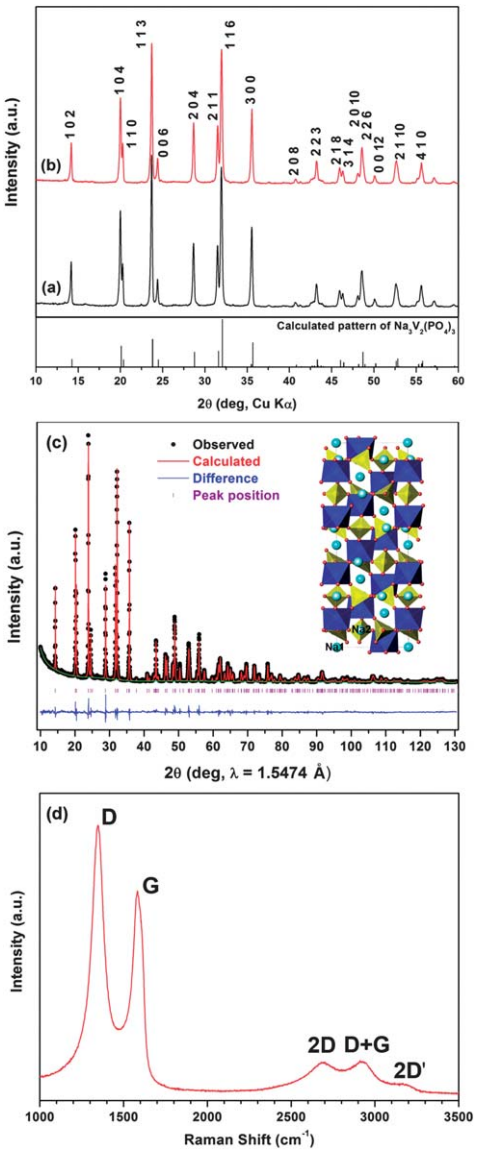

Fig. 1 The powder XRD patterns for (a) bare NVP and (b) the NVP/graphene composite. (c) The synchrotron diffraction data with Rietveld refinement for the NVP/graphene composite. The inset shows a crystal structure of $Na_3V_2(PO_4)_3$ projected along the [100] direction. (d) Raman spectrum of the NVP/graphene composite.

the Na2 site is occupied; hence, full stoichiometry of Na is 3 in NASICON structured NVP. However, our Rietveld refinement results indicate that Na ions are accommodated in both Na1 and Na2 sites with partial occupancy. This result is in agreement with a recent report about NVP.[33] Additionally, bond valence sums (BVS) were calculated with the program VALENCE[34] to confirm the expected charges of the ions based on the Rietveld refinement results. The BVS result for the V atom is 3.13, suggesting close to V^{3+} in the NASICON phase.

Raman spectrum shows the presence of the D (1347 cm^{-1}) and G (1581 cm^{-1}) bands in the NVP/graphene arising from the characteristic graphite-like materials as shown in Fig. 1(d). In addition, weak peaks at 2692, 2928, 3170 cm^{-1} are also observed, which are generally assigned as the 2D, D + G, and 2D′ of reduced graphene oxide, respectively.[35] The intensity ratio between the D- and G-bands (I_D/I_G) in the NVP/graphene composite is around 1.28, indicating the reduced state of graphene by thermal treatment during solid state synthesis under a reducing atmosphere (N_2–H_2 mixture). The lower intensity in the G band can be ascribed to the support of NVP particles on graphene surfaces, which might be induced by the interaction between particles and graphene. It also should be noted that the graphene sheet was not detected in the SPXRD data. If synthesized particles are randomly distributed on basal planes composed of irregular layer-stacked graphene sheets, it is difficult to detect graphene diffraction peaks.[36] Moreover, it indicates that the aggregation of graphene layers could be suppressed by our synthetic approach in spite of the high-temperature (700 °C) reaction.

To verify the graphene sheets, both SEM and TEM analyses were performed. No clear differences in primary particle size and morphology are apparent between the two samples, but the graphene sheets were observed as shown in Fig. 2(a) and (b). The primary particle size is approximately hundreds of nanometers, and the particles are agglomerated. In Fig. 2(b), several exfoliated graphene sheets are clearly seen. A TEM image (Fig. 2(c)) more clearly shows that NVP particles were successfully grown on graphene surfaces. Fig. 2(d) also indicates the high crystallinity of the NVP/graphene composite, and the interplanar *d*-spacing and SAED patterns are in good agreement with the (024) and (113) planes for the rhombohedral NASICON NVP as indicated in Fig. 2(e) and (f). It is suggested that a NVP/graphene composite can be synthesized using the following three steps: (1) growth of amorphous vanadium oxide nanoparticles on a graphene oxide surface, (2) NVP precursor homogeneous mixing and gelation, and (3) crystallization through a high-temperature solid-state reaction and simultaneous thermal reduction of graphene oxide. As a chelating agent, oxalic acid is the likely source of amorphous carbon after high-temperature synthesis under a reducing atmosphere, which is consistent with previous reports,[11,12,29] and oxalic acid may prevent particle growth during the high-temperature reaction. Further, oxalic acid plays a role as a reductant to reduce V^{5+} to V^{3+} during the heat treatment process under N_2 mixed 5% H_2 which is a reductant as well. H_2 is considered as a reducing agent for GO and for preventing oxidation of V^{3+}.

The electrochemical performances of bare NVP and the NVP/graphene composite in Na half-cells are compared in Fig. 3. All gravimetric capacity of the NVP/graphene composite is calculated based on the total weight of the composite which contains approximately 5 wt% of graphene. The 0.2 C charge–discharge voltage profiles show a flat potential plateau at approximately 3.4 V, which indicates a two-phase reaction corresponding to the redox couple of $V^{4+/3+}$ and is in good agreement with the previous experimental results.[11–13,28,29] The initial coulombic efficiency of two samples is around 94%, a relatively low value may be attributed to the kinetic barriers by structural changes during Na de/insertion.[12] Furthermore, other groups have also observed low coulombic efficiency of NVP in PC electrolytes at low C-rates.[11–13] This tendency in NASICON-structured NVP has not been completely explained yet, but the optimization of Na-ion cells with suitable electrolyte systems could alleviate this issue.[28]

Although the two samples have similar crystallinity, morphology and a same $Na_3V_2(PO_4)_3$ phase, the high-rate performances for the two samples are entirely different. The NVP/graphene composite delivers the discharge capacities of 90.6, 90.2, 89.5, 88.2, 86.3, 83.5, 74.4 and 60.4 mA h g^{-1} at 0.2, 0.5, 1, 2, 5, 10, 20 and 30 C, respectively, whereas bare NVP delivers the discharge capacities of 93.6, 90.0, 83.7, 72.3, 43.2 and 0.9 mA h g^{-1} at 0.2, 0.5, 1, 2, 5 and 10 C, respectively (Fig. 3(a) and (b)). It is apparent that the voltage polarization of

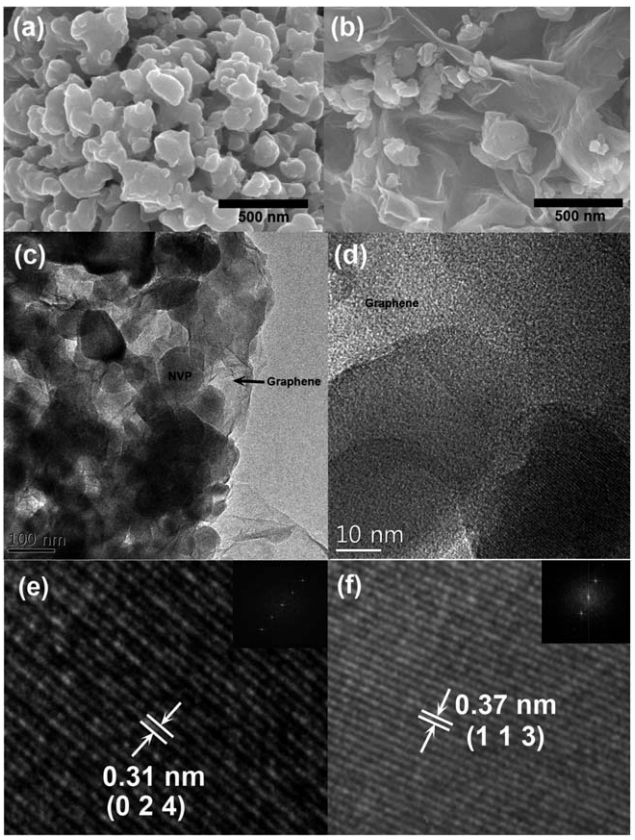

Fig. 2 SEM images of (a) bare NVP and (b) the NVP/graphene composite. (c) A TEM image and (d) an HRTEM image of the NVP/graphene composite. Magnified HRTEM images and SAED patterns of the (e) (0 2 4) plane and (f) (113) plane.

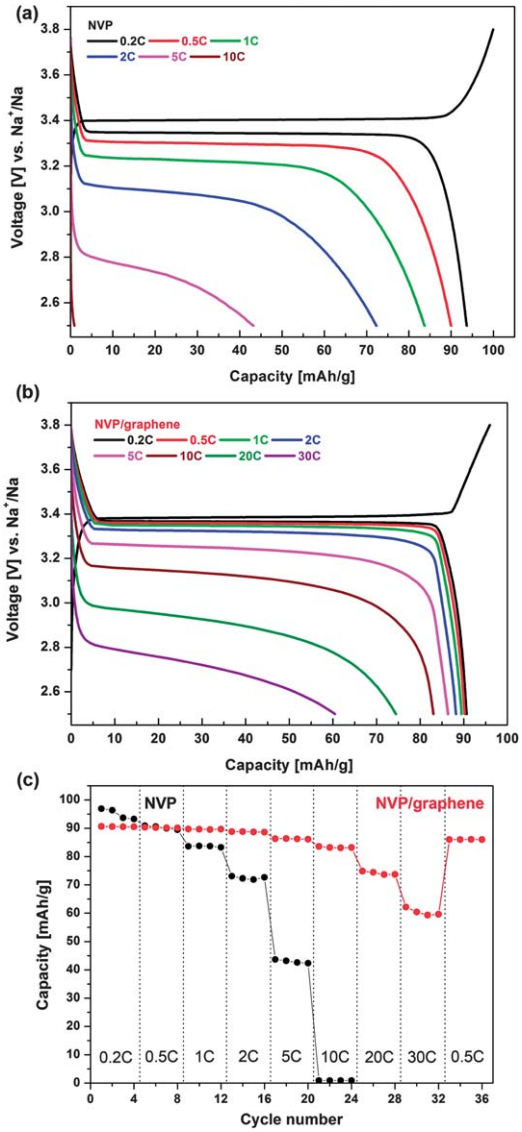

Fig. 3 The discharge profiles at various C-rates for (a) bare NVP and (b) the NVP/graphene composite. (c) Capacity retention at different C-rates for bare NVP and the NVP/graphene composite, respectively. The charge rate was fixed at 0.2 C.

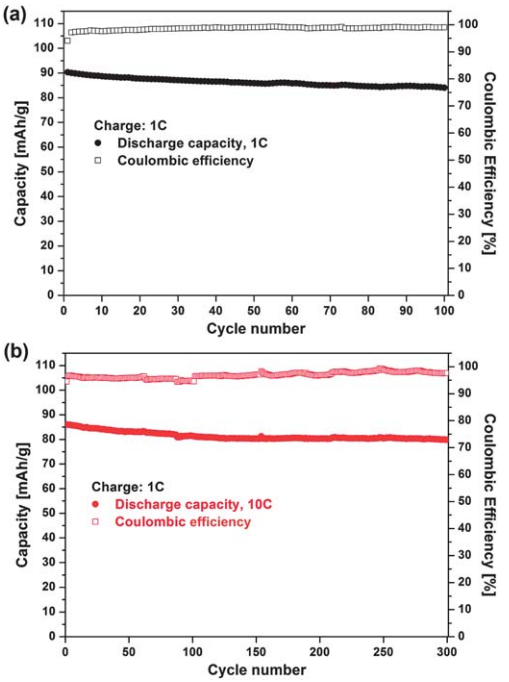

Fig. 4 Specific capacity and coulombic efficiency for the NVP/graphene composite during cycling at a rate of (a) 1 C and (b) 10 C.

the composite between the charge and discharge curves is appreciably lower than that of bare NVP, even at a low C-rate. While the first discharge capacity is slightly diminished due to the total weight of the composite (containing around 5 wt% of graphene), the NVP/graphene composite exhibits outstanding capacity retention at high C-rates compared with bare NVP as shown in Fig. 3(c). It is noted that the initial capacity of the NVP/graphene composite is almost attained when the current rate returns to 0.5 C after discharging at high C-rates. It could be speculated that graphene sheets are likely an embedded support in an electronic conducting path for the composite;[31] hence, the graphene composite can be effective in enhancing the electronic conductivity of $Na_3V_2(PO_4)_3$. As a result, it could have produced excellent results in a high C-rate test.

Fig. 4(a) shows the specific capacity of the NVP/graphene composite during cycling at 1 C of charge and discharge. The capacity retention is approximately 93% of its initial specific capacity after 100 cycles. Good cycleability means a stable crystal framework in the NASICON structure. To demonstrate lifetime of the NVP/graphene composite under severe conditions, the discharge capacity variation for the NVP/graphene composite was tested at a higher discharge rate of 10 C (Fig. 4(b)). The specific capacity is also maintained at approximately 80 mA h g^{-1} after 300 cycles of 10 C discharge.

Conclusions

We present a simple synthetic approach for attaching $Na_3V_2(PO_4)_3$ to graphene surfaces and enhancing rate performance in electrode materials. Both bare NVP and a NVP/graphene composite were synthesized with high crystallinity in sub-micron sized particles, and they deliver similar discharge capacities and voltage profiles at low C-rates; however, a dramatic gap in capacity between the two samples was observed at higher C-rates. The NVP/graphene composite delivers approximately 86 mA h g^{-1} of reversible capacity at 5 C with small polarization (~0.15 V) between charge and discharge. However, the bare NVP sample generated a worse performance with large polarization and delivered only approximately 43 mA h g^{-1} at the same C-rate. This composite also exhibits high capacity retention at both 1 C and 10 C cycles; thus, it is a promising cathode material for rechargeable sodium-ion batteries. The strategy herein for producing cathode materials with high-rate performances and long lifetimes promotes the development of sodium-ion batteries; such applications could be broadened for sodium-based rechargeable batteries.

Acknowledgements

This work was supported by the Program to Solve Climate Changes (NRF-2010-C1AAA001-2010-0029031) and Basic Science Research Program (2009-0094038) through the National Research Foundation of Korea (NRF) funded by the Ministry of Education, Science and Technology. The authors thank the Pohang Light Source, Korea for extending the synchrotron XRD for characterization.

Notes and references

1 B. Dunn, H. Kamath and J.-M. Tarascon, *Science*, 2011, **334**, 928.
2 T.-H. Kim, J.-S. Park, S. K. Chang, S. Choi, J. H. Ryu and H.-K. Song, *Adv. Energy Mater.*, 2012, **2**, 860.
3 J.-M. Tarascon, *Nat. Chem.*, 2010, **2**, 510.
4 S.-W. Kim, D.-H. Seo, X. Ma, G. Ceder and K. Kang, *Adv. Energy Mater.*, 2012, **2**, 710.
5 V. Palomares, P. Serras, I. Villaluenga, K. B. Hueso, J. Carretero-Gonzalez and T. Rojo, *Energy Environ. Sci.*, 2012, **5**, 5884.
6 M. D. Slater, D. Kim, E. Lee and C. S. Johnson, *Adv. Funct. Mater.*, 2013, **23**, 947.
7 M. D'Arienzo, R. Ruffo, R. Scotti, F. Morazzoni, C. M. Mari and S. Polizzi, *Phys. Chem. Chem. Phys.*, 2012, **14**, 5945.
8 M. Sathiya, K. Hemalatha, K. Ramesha, J.-M. Tarascon and A. S. Prakash, *Chem. Mater.*, 2012, **24**, 1846.
9 Y. H. Jung, S.-T. Hong and D. K. Kim, *J. Electrochem. Soc.*, 2013, **160**, A897.
10 S.-M. Oh, S.-T. Myung, J. Hassoun, B. Scrosati and Y.-K. Sun, *Electrochem. Commun.*, 2012, **22**, 149.
11 Z. Jian, L. Zhao, H. Pan, Y.-S. Hu, H. Li, W. Chen and L. Chen, *Electrochem. Commun.*, 2012, **14**, 86.
12 S. Y. Lim, H. Kim, R. A. Shakoor, Y. Jung and J. W. Choi, *J. Electrochem. Soc.*, 2012, **159**, A1393.
13 J. Kang, S. Baek, V. Mathew, J. Gim, J. Song, H. Park, E. Chae, A. K. Rai and J. Kim, *J. Mater. Chem.*, 2012, **22**, 20857.
14 Y. Kawabe, N. Yabuuchi, M. Kajiyama, N. Fukuhara, T. Inamasu, R. Okuyama, I. Nakai and S. Komaba, *Electrochem. Commun.*, 2011, **13**, 1225.
15 J. Ding, Y. Zhou, Q. Sun and Z. Fu, *Electrochem. Commun.*, 2012, **22**, 85.
16 J. Qian, M. Zhou, Y. Cao, X. Ai and H. Yang, *Adv. Energy Mater.*, 2012, **2**, 410.
17 A. K. Geim, *Science*, 2009, **324**, 1530.
18 M. J. Allen, V. C. Tung and R. B. Kaner, *Chem. Rev.*, 2010, **110**, 132.
19 Y. Sun, Q. Wu and G. Shi, *Energy Environ. Sci.*, 2011, **4**, 1113.
20 D. Chen, H. Feng and J. Li, *Chem. Rev.*, 2012, **112**, 6027.
21 G. Kucinskis, G. Bajars and J. Kleperis, *J. Power Sources*, 2013, **240**, 66.
22 J. B. Goodenough, H. Y.-P. Hong and J. A. Kafalas, *Mater. Res. Bull.*, 1976, **11**, 203.
23 C. Delmas, A. Nadiri and J. L. Soubeyroox, *Solid State Ionics*, 1988, **28–30**, 419.
24 H. Aono, E. Sugimoto, Y. Sadaoka, N. Imanaka and G. Adachi, *J. Electrochem. Soc.*, 1993, **140**, 1827.
25 J. Gaubicher, C. Wurm, G. Goward, C. Masquelier and L. Nazar, *Chem. Mater.*, 2000, **12**, 3240.
26 B. L. Cushing and J. B. Goodenough, *J. Solid State Chem.*, 2001, **162**, 176.
27 L. S. Plashnitsa, E. Kobayashi, Y. Noguchi, S. Okada and J. Yamaki, *J. Electrochem. Soc.*, 2010, **157**, A536.
28 Z. Jian, W. Han, X. Lu, H. Yang, Y.-S. Hu, J. Zhou, Z. Zhou, J. Li, W. Chen, D. Chen and L. Chen, *Adv. Energy Mater.*, 2013, **3**, 156.
29 K. Saravanan, C. W. Mason, A. Rudola, K. H. Wong and P. Balaya, *Adv. Energy Mater.*, 2013, **3**, 444.
30 W. S. Hummers and R. E. Offeman, *J. Am. Chem. Soc.*, 1958, **80**, 1339.
31 C. H. Lim, A. G. Kannan, H.-W. Lee and D. K. Kim, *J. Mater. Chem. A*, 2013, **1**, 6183.
32 A. C. Larson and R. B. Von Dreele, *GSAS, Report LAUR 86–748*, Los Alamos National Laboratory, New Mexico, USA, 2000.
33 I. V. Zatovsky, *Acta Crystallogr., Sect. E: Struct. Rep. Online*, 2010, **66**, i12.
34 C. Hormillosa, S. Healy, T. Stephen and I. D. Brown, *Bond Valence Calculator, Version 2.0*, McMaster University, Canada, 1993.
35 R. Liang, H. Cao, D. Qian, J. Zhangc and M. Qu, *J. Mater. Chem.*, 2011, **21**, 17654.
36 J. Zhang, Z. Xiong and X. S. Zhao, *J. Mater. Chem.*, 2011, **21**, 3634.

